Radiation Measurements 71 (2014) 8–14

Contents lists available at ScienceDirect

Radiation Measurements

journal homepage: www.elsevier.com/locate/radmeas

The role of simulations in the study of thermoluminescence (TL)

Reuven Chen [a,*], Vasilis Pagonis [b]

[a] Raymond and Beverly Sackler School of Physics and Astronomy, Tel Aviv University, Tel Aviv 69978, Israel
[b] Physics Department, McDaniel College, Westminster, MD 21157, USA

HIGHLIGHTS

- Simulations of OTOR TL peaks using solution of sets of simultaneous differential equations.
- Evaluation of effective activation energies and frequency factors.
- Study of very high activation energies and frequency factors.
- Study of very low activation energies and frequency factors.

ARTICLE INFO

Article history:
Received 13 October 2013
Received in revised form
20 December 2013
Accepted 23 December 2013
Available online 10 January 2014

Keywords:
Thermoluminescence (TL)
Optically stimulated luminescence (OSL)
Simulations

ABSTRACT

The traffic of charge carriers in a luminescent material during its excitation by irradiation and during readout either in the measurement of thermoluminescence (TL) or optically stimulated luminescence (OSL) is governed by sets of coupled nonlinear differential equations. The analytical solution of these sets is usually not possible, and one can resort to one of two options. Some researchers preferred to make simplifying assumptions and thus got approximate solutions whereas others performed simulations by solving the simultaneous equations numerically. Each of these routes has its pitfalls. The simplifying assumptions, mainly the quasi-equilibrium assertion or the assumption that certain relations between the relevant parameters and functions hold, may be valid in certain ranges of the TL or OSL curve, and may cease to be valid, say at the high-temperature range in TL. Performing simulations using the numerical solution of the relevant set of equations may yield results which are accurate, but cannot be considered as being general because they depend on the specific choice of the parameters. Repeating the simulations with several sets of the physically plausible parameters would add credibility to the conclusions drawn. The combination of the two approaches is highly recommended, i.e, if similar results are found by approximations and simulations, the validity of the conclusions is strengthened. Evidently, the comparison of these theoretical results to experimental effects is essential. In the present work we consider the occurrence of unusually high and unusually low values of the activation energy and the effective frequency factor. In particular, we can simulate a recently discovered behavior of TL in LiF:Mg, Cu, P at the ultra-high dose range and get qualitatively the main elements of the experimentally found results.

1. Introduction

The processes of thermoluminescence (TL) and optically stimulated luminescence (OSL) involve in most cases the excitation by irradiation of electrons from the valence band into the conduction band, followed by their capture in electron traps associated with imperfections in the lattice, impurities or defects. The holes remaining in the valence band may be trapped in hole centers which are associated with different kinds of imperfections. This stage of excitation is followed by relaxation, a period of time in which the sample is held in the dark and in ambient temperature, and the remaining free electrons and holes may still be captured by traps and centers. The third stage of read-out follows, in which the sample is either heated up, in TL, or illuminated by, say, IR light in OSL. Here, the trapped electrons are released, usually into the conduction band, and may perform radiative recombination with holes in centers thus producing measurable luminescence, as a function of temperature in TL or of time in OSL.

In the simplest case of one trap and one recombination center (OTOR) the situation is a simplified version of the schematic energy level diagram in Fig. 1, with $K = 1$, one trapping state and $L = 1$, one kind of recombination center. In the more realistic and complex

* Corresponding author. Tel.: +972 9 9553276; fax: +972 9 9561213.
E-mail address: chenr@tau.ac.il (R. Chen).

1350-4487/$ – see front matter © 2014 Elsevier Ltd. All rights reserved.
http://dx.doi.org/10.1016/j.radmeas.2013.12.011

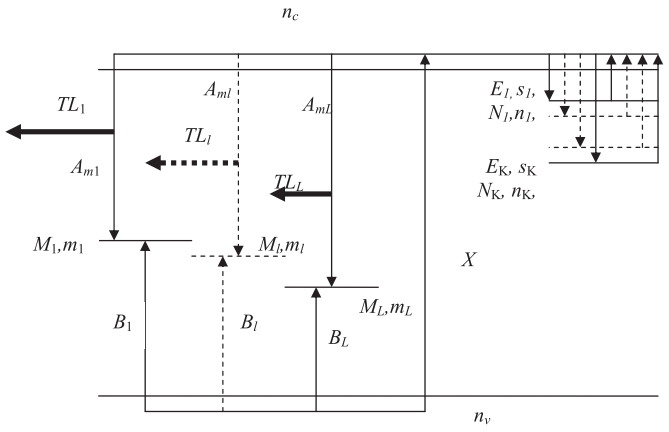

Fig. 1. Schematic energy-level diagram with K trapping states (N_i) and L kinds of recombination center (M_l). Transitions occurring both during excitation and during heating are shown. The dashed lines signify that these levels and transitions represent multiple levels/transitions of the same kind. The thick arrows denote the possible different TL emissions.

situations, several trapping states are involved, $K > 1$, and a number of recombination centers, $L > 1$, as shown in Fig. 1. The relevant sets of coupled differential equations, which will be given below, are sets of non-linear equations and as such, are usually not amenable to analytical solutions. Solving these equations is, however, crucial in understanding the processes involved and in trying to explain the wealth of effects, some of which are anomalous at first sight. Sometimes the results of such solution may help in predicting some new phenomena.

Two alternative ways to deal with these sets of equations have been offered in the literature. Many authors resorted to the use of simplifying assumptions and thus found approximate analytical expressions which led under the appropriate conditions to the well known first-order and second-order kinetics. One may question, however, the validity or at least the range of applicability of the simplifying assumptions used. An alternative, viable route, which became more accessible with the development of fast computers and availability of very efficient software for the solution of simultaneous differential equations, is the use of simulations. Here, one may choose a set of physically acceptable trapping parameters and solve the relevant sets of equations in a sequence which simulates the experimental steps of the procedure. In most cases, this can be performed with any desirable accuracy. The main deficiency of this method is that with the choice of specific sets of parameters, it is very hard to come to general conclusions. A partial solution is to repeat the numerical procedure for several sets of the parameters, and try to draw conclusions from the accumulation of the results. In general, it is possible to demonstrate by simulations that certain phenomena seen in experiments are commensurate with the chosen model and sets of parameters. For example, non-linear dependence of TL or OSL intensity on the dose of excitation or the possibility of dependence of the emitted luminescence on the dose-rate of excitation could be demonstrated by simulations and in some cases could be explained more intuitively in parallel.

In the present paper we first present briefly the models consisting of trapping states and centers, and follow the flow of carriers between them and the conduction and valence bands during the different stages of excitation-relaxation-readout. Different sequences of the experimental procedure are followed in an attempt to explain various aspects of TL and OSL measurements.

2. The models

A rather general energy level scheme with several trapping states and a number of recombination centers is shown in Fig. 1. The diagram shows both the transitions taking place during excitation and heating (in TL) or illumination (in OSL) during read-out. The diagram shows K trapping states and L recombination centers. The rate of production of electrons and holes is denoted by X, which is proportional to the dose-rate of excitation.

Let us consider first the simplest situation of one trapping state and one kind of recombination center, i.e., $K = L = 1$. This is the mentioned case of one-trap-one recombination center (OTOR). The set of simultaneous differential equations governing the process during excitation in this case is (see e.g., Chen et al., 1981):

$$\frac{dn}{dt} = A_n(N-n)n_c, \tag{1}$$

$$\frac{dm}{dt} = B(M-m)n_v - A_m m n_c, \tag{2}$$

$$\frac{dn_v}{dt} = X - B(M-m)n_v, \tag{3}$$

$$\frac{dn_c}{dt} = X - A_n(N-n)n_c - A_m m n_c. \tag{4}$$

Here, N and M are, respectively, the concentrations of traps and centers (cm^{-3}), n and m their instantaneous occupancies (cm^{-3}), n_c (cm^{-3}) and n_v (cm^{-3}) are the concentrations of free electrons and holes, respectively, A_m and A_n are, respectively, the recombination and retrapping probability coefficients of electrons ($cm^3\ s^{-1}$) and B is the trapping probability coefficient of free holes into centers ($cm^3\ s^{-1}$). If the process of irradiation takes place for a time t_D (s), the total concentration of electrons and holes produced during excitation is given by $D = X \cdot t_D$, where D denotes the dose or rather, it is proportional to the imparted dose.

The set of differential equations governing the process during the heating of the sample in a TL measurement, following excitation has been first given by Halperin and Braner (1960):

$$\frac{dn}{dt} = A_n(N-n)n_c - s \cdot n \cdot \exp(-E/kT), \tag{5}$$

$$I(T) = -\frac{dm}{dt} = A_m m n_c, \tag{6}$$

$$\frac{dn_c}{dt} = s \cdot n \cdot \exp(-E/kT) - A_n(N-n)n_c - A_m m n_c, \tag{7}$$

where E (eV) is the activation energy, s (s^{-1}) the frequency factor and k (eV K^{-1}) is the Boltzmann constant. Halperin and Braner (1960) studied the heating stage and made the simplifying assertion, later termed the "quasi-equilibrium" assumption

$$\frac{dn_c}{dt} \approx 0. \tag{8}$$

It is quite obvious that the condition (8) does not mean that $dn_c/dt = 0$ simply because $n_c(t)$ varies along the time of heating. Most authors agreed that the meaning of this condition is (see e.g. Dussel and Bube, 1967; Kelly and Bräunlich, 1970),

$$\left|\frac{dn_c}{dt}\right| << \left|\frac{dn}{dt}\right|;\ \left|\frac{dm}{dt}\right|. \tag{9}$$

A further discussion on the meaning of Eq. (8) and the validity of conditions (9) has recently been given by Chen and Pagonis (2013). Halperin and Braner (1960) have shown that Eqs. (5–7) can be simplified, by the use of the condition (8) along with assuming that $n_c << n$, and yield

$$I_{app}(T) = -\frac{dm}{dt} = s \cdot n \cdot \exp(-E/kT) \frac{A_m m}{A_m m + A_n(N-n)}. \quad (10)$$

Further simplifying assumptions lead to the well known first-order kinetics (Randall and Wilkins, 1945) and second-order kinetics (Garlick and Gibson, 1948).

A substantial extension of the model has to do with considering the simultaneous transitions between several trapping states and a number of recombination centers as shown in Fig. 1. The set of equations governing the read-out process is

$$\frac{dn_i}{dt} = A_i(N_i - n_i)n_c - s_i \cdot n_i \cdot \exp(-E_i/kT), \quad \text{for } i = 1 \ldots K \quad (11)$$

$$I_l(T) = -\frac{dm_l}{dt} = A_{ml} m_l n_c, \quad \text{for } l = 1, \ldots, L \quad (12)$$

$$\frac{dn_c}{dt} = \sum_{i=1}^{K} s_i n_i \exp(-E_i/kT) - \sum_{i=1}^{K} A_i(N_i - n_i)n_c - \sum_{l=1}^{L} A_{ml} m_l n_c. \quad (13)$$

Here, the i-th trap has activation energy of E_i, frequency factor s_i, concentration N_i, instantaneous occupancy n_i and retrapping probability coefficient A_i. The l-th hole center has instantaneous concentration m_l and recombination probability coefficient A_{ml}. Concerning Eq. (12), one should note that the relevant recombinations may or may not be radiative. In some cases, in order to explain certain effects we may assume that only one of these transitions is radiative and the others act as competitors that may contribute to the rather intricate processes taking place during heating. Alternatively, even if the competing centers are radiative but in a different range of the spectrum, the emissions can be separated by a spectrometer or by optical filters and only one emission may be dominant in the measured TL or OSL.

3. Anomalous values of trapping parameters found in TL measurements

In the analysis of TL in several materials, anomalous values of the activation energy and frequency factor, sometimes very high and sometimes very low, have been found in peaks, some of which having first-order symmetry.

First-order thermoluminescence (TL) peaks are defined by two parameters, namely, the activation energy E(eV) and the frequency factor s(s^{-1}). The expression giving the peak of TL in this case is (see Randall and Wilkins, 1945)

$$I(T) = s n_0 \exp(-E/kT) \exp\left[(-s/\beta)\int_{T_0}^{T} \exp(-E/k\theta)d\theta\right], \quad (14)$$

where n_0(cm^{-3}) is the initial concentration of electrons, β(K s^{-1}) is the (constant) heating rate, T_0(K) and T(K) are the initial and current temperatures, respectively, θ is the running temperature between T_0 and T and k(eV K^{-1}) is the Boltzmann constant. In the initial-rise range of the curve, the argument of the second exponential is very small and therefore, the exponent is very close to unity and, anyway, it is nearly constant. Therefore, in this range, $I(T) \propto exp(-E/kT)$ and thus, if one plots $ln(I(T))$ as a function of $1/kT$, one expects a straight line in the initial-rise range with a slope of $-E$. In fact, this method of evaluating the activation energy is considered to be viable in a much broader range of cases beyond the simple first-order situation (see e.g., Garlick and Gibson, 1948).

A number of methods for the evaluation of the activation energy of a TL peak using its shape have been suggested in the literature. As an example, Chen (1969a,b) has offered the following formula for evaluating the activation energy of a first-order peak, based on the measurement of the maximum of the peak and its half width

$$E = 2.52kT_m^2/\omega - 2kT_m, \quad (15)$$

where T_m is the temperature at the maximum and $\omega = T_2 - T_1$ and where T_1 and T_2 are, respectively, the low and high half-width temperatures. Once the activation energy of a first-order peak is determined, the frequency factor can easily be determined by using the maximum condition

$$s = \frac{\beta E}{kT_m^2}\exp(E/kT_m). \quad (16)$$

As shown by several authors (e.g., Halperin and Braner, 1960), a first-order peak is characterized by an asymmetric shape; its fall-off part is narrower than the low-temperature increasing part. Chen (1969a) has shown that a typical value of the symmetry factor, $\mu_g = \delta/\omega$ (where $\delta = T_2 - T_m$) is, for a first-order peak ~0.42. Chen (1969b) has further shown that for a general-order peak, the activation energy can be evaluated by

$$E = \left[2.52 + 10.2\left(\mu_g - 0.42\right)\right]kT_m^2/\omega - 2kT_m. \quad (17)$$

3.1. The occurrence of very high activation energies and frequency factors

According to Mott and Gurney, s should be of the order of magnitude of the Debye frequency, which has to do with the number of times per second that the trapped electron interacts with the phonons. Indeed, many results reported by various authors over the years gave values of s in the range of 10^{10}–10^{13} s^{-1}. In some cases, anomalously high values of the frequency factor, accompanied by high values of the activation energy, were reported. Taylor and Lilley (1978) reported a frequency factor of 2×10^{20} s^{-1} and an activation energy of 2.06 eV of peak V of LiF:Mg,Ti (TLD-100). Even larger values were reported by Gorbics et al. (1967) and by Pohlit (1969). Fairchild et al. (1974) suggested that the kinetics of this peak and other peaks with unusually large s might be complicated and the apparent first-order behavior is an approximation of a more complex kinetics situation. Chen and Hag-Yahya (1996) presented a model of one trap and three recombination centers, one radiative and two non-radiative, to explain the possibility of high activation energy and very high frequency factor. They wrote the relevant sets of simultaneous differential equations for the excitation and heating stages and solved them numerically. As a result of the competition of the two radiationless centers, the apparent curve which simulates the measurable TL peak looks like a very narrow first-order peak. With regard to Eq. (15), this means that ω is very small and, as a result, the apparent activation energy is very high, around twice as large as the value inserted into the simulations. Once this high value is inserted into Eq. (16), the effective frequency factor is many orders of magnitude higher than the one used for the simulation. In an example given, the inserted parameters are $E = 1.2$ eV and $s = 2.5 \times 10^{11}$ s^{-1} and the evaluated

parameters are $E_{eff} = 2.24$ eV and $s_{eff} = 9.3 \times 10^{21}$ s^{-1}. Mandowski (2006) has offered another possible explanation to the occurrence of very high frequency factors and high activation energies in first-order-shaped TL peaks, which is based on the concept of cascade detrapping (CD).

In a recent set of papers (e.g., Bilski, et al., 2008), TL in LiF:Mg, Cu, P at the "ultra-high" dose range of up to ~1 MGy has been reported. These authors describe a TL peak occurring at the range of 420–480 °C. The peak is very narrow, and therefore it has very high evaluated activation energy and frequency factor (e.g. $E = 4.47$ eV; $s = 10^{28}$ s^{-1}). The other features of this peak are:

1. It shifts to higher temperature by up to 65 K with increasing dose.
2. The measured E and s increase with the dose.
3. The emission spectrum changes and new bands appear at up to 800 nm.

For a model with one trapping state and three recombination centers, one radiative and two non-radiative, we have chosen the following set of parameters. $E = 1.9$ eV; $s = 2.5 \times 10^{11}$ s^{-1}; $X = 10^{22}$ m^{-3} s^{-1}; $t_D = 20$ s; $B_1 = 10^{-21}$ m^3 s^{-1}; $B_2 = 1.1 \times 10^{-21}$ m^3 s^{-1}; $B_3 = 1.2 \times 10^{-21}$ m^3 s^{-1}; $N = 1.2 \times 10^{21}$ m^{-3}; $M_1 = 4 \times 10^{21}$ m^{-3}; $M_2 = 4 \times 10^{19}$ m^{-3}; $M_3 = 4 \times 10^{21}$ m^{-3}; $A_n = 10^{-22}$ m^3 s^{-1}; $A_{m1} = 1.2 \times 10^{-18}$ m^3 s^{-1}; $A_{m2} = 2.8 \times 10^{-19}$ m^3; $A_{m3} = 7.5 \times 10^{-20}$ m^3 s^{-1}. The results showing the peak representing the radiative transitions into M_2 are shown by the solid line in Fig. 2. Table 1 shows the variation of T_m, E_{eff}, s_{eff} and the symmetry factor μ_g for the set of parameters chosen and for times of excitation varying between 0.2 and 20 s. The dashed line in Fig. 2 represents the first-order peak evaluated by inserting effective values E_{eff} and s_{eff} from the last entry of Table 1 in the first-order Equation (14) (see discussion below).

The model and simulations yield the following features found experimentally by Obryk et al. (2011) in LiF:Mg, Cu, P:

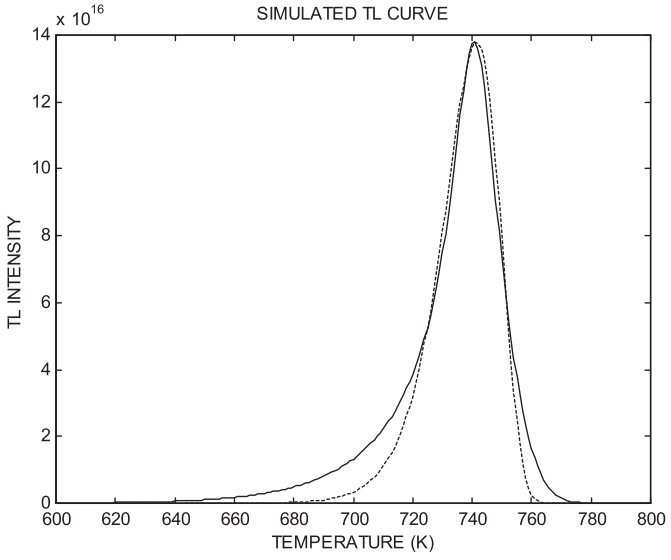

Fig. 2. An example of a simulated peak yielding very high effective activation energy and frequency factor. The parameters taken for the simulation are $E = 1.9$ eV; $s = 2.5 \times 10^{11}$ s^{-1}; $X = 10^{22}$ m^{-3} s^{-1}; $t_D = 20$ s; $B_1 = 10^{-21}$ m^3 s^{-1}; $B_2 = 1.1 \times 10^{-21}$; $B_3 = 1.2 \times 10^{-21}$; $N = 1.2 \times 10^{21}$ m^{-3}; $M_1 = 4 \times 10^{21}$ m^{-3}; $M_2 = 4 \times 10^{19}$ m^{-3}; $M_3 = 4 \times 10^{21}$ m^{-3}; $A_n = 10^{-22}$ m^3 s^{-1}; $A_{m1} = 1.2 \times 10^{-18}$ m^3 s^{-1}; $A_{m2} = 2.8 \times 10^{-19}$ m^3; $A_{m3} = 7.5 \times 10^{-20}$ m^3 s^{-1}. The solid line depicts the results of the numerical solution and the dashed line shows the first-order peak calculated using Eq. (14) with E_{eff} and s_{eff}.

Table 1
Results of evaluated parameters of a simulated peak from the one-trap three-center model.

t_D (s)	I_m (a.u.)	T_m (K)	μ_g	E_{eff} (eV)	s_{eff} (s^{-1})
0.2	4.60×10^{14}	720	0.418	1.91	9.63×10^{11}
0.5	3.21×10^{15}	722	0.444	2.64	1.57×10^{17}
1	1.03×10^{16}	728	0.457	3.66	1.66×10^{24}
2	2.55×10^{16}	733	0.464	4.79	8.55×10^{24}
3	3.94×10^{16}	735	0.462	5.14	2.06×10^{34}
5	6.23×10^{16}	738	0.417	4.73	2.16×10^{31}
10	1.00×10^{17}	740	0.409	5.04	2.22×10^{33}
20	1.38×10^{17}	741	0.409	5.05	2.48×10^{33}

1. Unusually high values of E_{eff} and s_{eff} are found following excitation at high dose.
2. The peak shifts to higher temperature with the dose.
3. These values increase further with increasing dose.
4. In many cases (but not always) the curve has symmetry of a first-order peak.

Practically the same results are found when the dose changes by changing the dose rate and by changing the time of excitation.

Obviously, the model is an oversimplification of a more complex situation. To begin with, it does not include the lower temperature peaks at all. Also, Obryk et al. (2011) report on a shift of the emission spectrum at the highest doses. In the model we have some interplay between transitions into different centers that may cause a change in the emission spectrum but as a first step, we have assumed that only one transition is radiative. Finally, the temperature shift is in the right direction but it amounts only to 21 K. Perhaps a refinement in the model is needed.

The parameters chosen for the simulations are in the reasonable physical range, but we do not claim that we know specifically that they really have to do with LiF:Mg, Cu, P. Thus, the results of the simulations are merely a demonstration that the experimentally observed unusual results can be explained qualitatively within the frame of the suggested model. It is quite obvious that in the real-life material, more traps and centers may be involved which will contribute to the complex phenomena observed.

3.2. *The occurrence of very low activation energies and frequency factors*

In the literature, there are also reports on very small frequency factors, accompanied by small activation energies. Haake (1957) reported results of activation energies and frequency factors of TL in ZnS·ZnO–Cu, Pb, Cl and ZnS–Cu, Cl, in which values of the frequency factor between 1 and 2×10^3 s^{-1} were found. They also mention previously found values of the frequency factor of TL in ZnS determined by Hoogenstraaten and Klasens (1953) and Dropkin (1954) in which the frequency factor s was found to be between 300 and 5×10^4 s^{-1}, again non-physically low values. Hickmott (1972) studied a TL peak at ~380 °C in sputtered SiO_2 films and found an activation energy of $E = 0.66$ eV and a frequency factor of $s \sim 10^4$ s^{-1}. Unusually low values of the activation energy and frequency factor have been reported for the associated effect of thermally stimulated conductivity (TSC).

Bräunlich (1967) and Sunta et al. (1999) pointed out that within the one-trap-one-recombination-center model (OTOR), if retrapping is strong and if the traps are filled to saturation, the standard initial-rise method as well as the peak-shape methods and glow-peak fitting yield very low effective values of the activation energy. Bräunlich (1967) showed by numerical solution of the relevant set of differential equations that for saturated trap and A_n/

$A_m \sim 1000$ where A_n is the retrapping probability coefficient and A_m the recombination probability coefficient, the initial-rise method yields a value of $\sim 0.43E$ where E is the real activation energy. Sunta et al. (1999) tested two models, OTOR and interactive multitrap system (IMTS) in which the occurrence of an additional thermally disconnected deeper trap (TDDT) is assumed. Using the peak shape methods (similar to Eq. (15) above) as well as a best-fit method, they found for cases of saturated trap and high retrapping low values of the effective activation energy down to $\sim 0.466E$. These authors have not dealt with the effective frequency factor, but it is obvious that in this case, the effective frequency factor found by Eq. (16) would be several orders of magnitude lower than the "real" one.

In the present work we add some insight to the underlying reasons for the possibility of getting unusually low values of the activation energy and frequency factor under the mentioned circumstances. Let us consider the following situation with regard to Eq. (10). Going along with the assumptions made by Bräunlich (1967) and by Sunta et al. (1999), we consider the case where retrapping dominates and the traps are saturated at the beginning of heating. At the very beginning of the peak in question, since the trap is saturated, $A_n(N-n)$ is nil, and the simple first-order equation holds. However, as temperature increases, n decreases and therefore $N-n$ increases. Since A_n is assumed to be very large, $A_n(N-n)$ increases very quickly and surpasses $A_m m$. Therefore, the simple first-order expression in Eq. (10), $s \cdot n \cdot exp(-E/kT)$ is multiplied by a very fast decreasing function of temperature. This fast decreasing function is shown in Fig. 3 on a linear scale and in Fig. 4 on a logarithmic scale, in the results of numerical simulation (details are given below). As seen in the latter, it may be approximated by an exponential function, $\sim \exp(E_e/kT)$ where E_e(eV) is an effective energy in the vicinity of $E/2$. If this approximation is added to Eq. (10), the result is a first-order equation of the form

$$I(T) = -\frac{dn}{dt} = s \cdot n \cdot \exp[-(E-E_e)/kT]. \quad (18)$$

It is quite obvious that the solution of this equation is a first-order peak with effective activation energy of $E - E_e$. This can be expected to be seen both in the initial-rise method and in the peak-shape methods; in view of Eq. (15), it is clear that the width of the peak should be rather large in line with the low effective value of the activation energy. It should be noted that since the expression $A_m m/[A_m m + A_n(N-n)]$ is only approximately exponential with temperature (see below), its deviation from simple exponential may result in an appearance of the glow peak which differs from pure first order. The reduction function varies by $\sim e^8 \sim 3000$ in the relevant temperature range. This is a very significant variation, and although the function is not exactly exponential, it explains qualitatively the significant reduction in the effective activation energy and frequency factor under these circumstances.

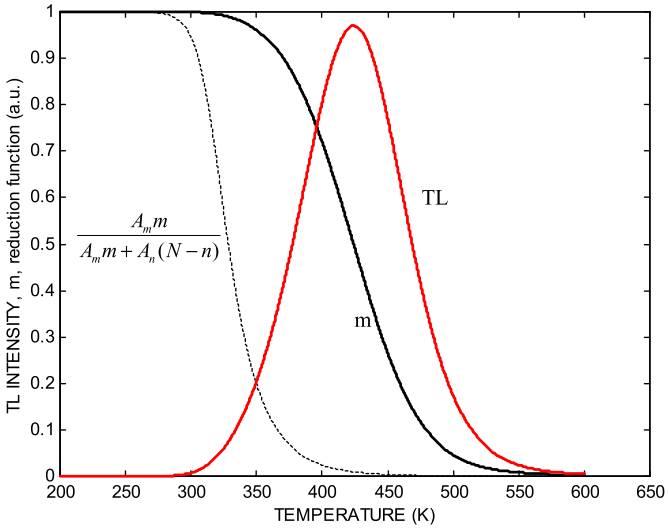

Fig. 3. Simulated TL peak with high retrapping coefficient following excitation to saturation, within the OTOR model. The parameters used are $n_0 = m_0 = N = 10^{16}$ m^{-3}, $s = 10^{11}$ s^{-1}; $E = 0.9$ eV, $A_m = 10^{-15}$ m^3 s^{-1}, $A_n = 10^{-13}$ m^3 s^{-1}. TL represents the thermoluminescence curve, $m(T)$ is the concentration of holes in the center and $A_m m/A_m m + A_n(N-n)$ is the reduction function.

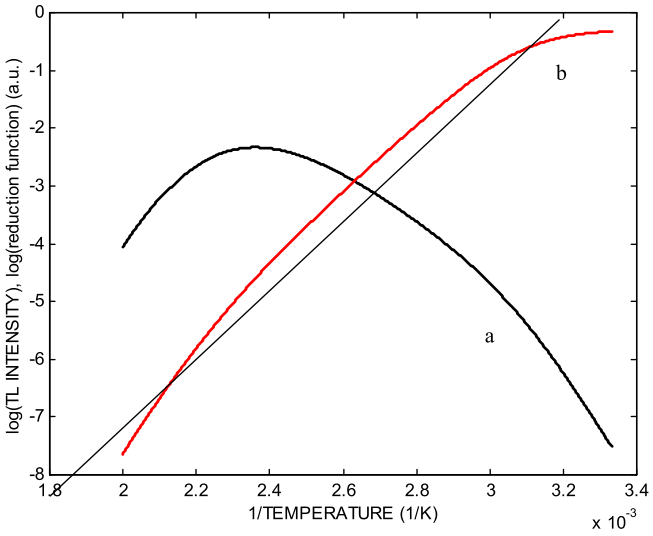

Fig. 4. The same results except that the x-axis is given in inverse temperature and the y-axis is logarithmic. Curve (a) is the TL peak and curve (b), the reduction function. The straight line is a rough approximation of the reduction function which represents an approximate exponential behavior of this magnitude.

In order to demonstrate the described situation of TL with strong retrapping and initial filling of the traps to saturation, Eqs. (5–7) were solved numerically using an appropriate set of parameters. The parameters chosen were $n_0 = m_0 = N = 10^{16}$ m^{-3}, $s = 10^{11}$ s^{-1}; $E = 0.9$ eV, $A_m = 10^{-15}$ m^3 s^{-1}, $A_n = 10^{-13}$ m^3 s^{-1} and the heating rate was $\beta = 1$ K/s. The curves shown in Fig. 3 are of simulated TL as a function of temperature with a maximum at 424 K, as well as m and the "reduction function" $A_m m/A_m m + A_n(N-n)$, both normalized to unity, as a function of temperature. It is readily seen that the reduction function decreases from unity to zero in the temperature range between ~ 275 K and ~ 400 K whereas normalized m decreases from unity to zero between ~ 320 K and ~ 540 K. The fast decrease of the reduction function in the range of the TL peak's initial-rise and low-temperature half can explain the unusually low values of the activation energy and frequency factor.

Analysis of the TL curve shows in this case a value of the symmetry factor μ_g of 0.488, roughly similar to results given by Sunta et al. (1999), and an activation energy calculated from Eq. (15) of 0.46 eV.

In order to check the assertion made above that the reduction function behaves approximately like an exponential of the form $\sim exp(E_e/kT)$, a plot of the same results in the form of natural logarithm vs. $1/T$. This is shown in Fig. 4. Curve (a) shows the simulated glow peak on this scale and curve (b) is the reduction function. The straight line is an approximation of curve (b), and its slope is in accordance with energy of $E_e \sim 0.5$ eV. The possible consequences of the deviation of the straight line from curve (b) are discussed below.

We have also retrieved the activation energy by the initial rise method from the simulated TL curve in Fig. 3. Some results are shown in Table 2. Since the values of the TL are numerically simulated, namely with no experimental noise, it has been sufficient to choose for each evaluation two points rather close to each other and the apparent initial-rise energy was determined by

$$E = k \ln\left(\frac{I_2}{I_1}\right) \frac{T_1 T_2}{T_2 - T_1}, \tag{19}$$

where T_1, T_2 are the two chosen temperatures and I_1, I_2 the two respective intensities. The temperature values in Table 2 stand for T_1 and $T_2 = T_1 + 5$. Note that I(344 K) is about 5% of the maximum intensity, I(368 K) about 10% of the maximum whereas 281 K and 301 K are at the very low end of the peak where the intensities are only a small fraction of the maximum intensity. In most cases, in real experimental results, such small intensities are not measurable, and the initial-rise values are usually estimated in the 5–10% intensity range (see e.g. Chen and Haber, 1968). The occurrence of the "real" initial-rise activation energy only at the very low range of temperatures under similar conditions has been mentioned by Bräunlich (1967). The underlying reasons for these results are discussed below.

4. Discussion

Concerning the case of very high activation energy and frequency factor discussed in sub Section 3.1, with regard to the shape of the peak shown in Fig. 2, one should consider the similarity between the simulated peak found by solving Eqs. (1–4) followed by the solution of Eqs. (5–7), and the pure first-order peak with the E_{eff} and s_{eff} values found by the conventional analysis of the simulated peak. As could be expected, the two peaks occur at the same temperature, have practically the same width and the same symmetry factor determined by the temperatures at the maximum and at half intensity. In the range between ~725 K and 755 K, the two curves are very close together. At the low temperature and high temperature ranges, the simulated curve deviates from the first-order curve. This should not be very surprising. The one trap-three center system is significantly more complex, and whereas the existence of the two additional radiationless centers can explain the occurrence of a narrow peak with a first-order-like symmetry, yielding very high effective values of E and s, there is no claim that the two curves should coincide all along.

As pointed out above, the results of Table 1 show that at least qualitatively, the intriguing results by Obryk et al. (2011) can be explained by the given model. Note that in the results of Table 1, the first-order symmetry occurs at the lower and higher doses of excitation, whereas in the middle doses (between 1 and 3 s of simulated excitation), the symmetry factor resembles that of ~1.4 order TL peak. In these cases, the effective value of the activation energy was evaluated by Eq. (17) rather than Eq. (15).

As for the described possibility of occurrence of very low activation energy and frequency factor, it is quite obvious from Figs. 3 and 4 that the "reduction function" changes very significantly in the range where the TL peak occurs. As pointed out, this has to do with the very fast increase of the term $A_n(N - n)$ which is in the denominator. Had this fast decrease with temperature (fast increase with $1/T$) been exponential, the shown function would have coincided with the straight line and the effective activation energy, both by the peak-shape methods and the initial-rise method, would have been $E - E_0$. With $E = 0.9$ eV and the slope of the straight line commensurate with $E_0 = 0.5$ eV, the effective activation energy would be expected to be 0.4 eV. Since the straight line is merely a rough estimate of the real curve, it is not surprising that the value we got by the peak-shape method is 0.46 eV and the initial-rise value is ~0.42 eV at ~344 K, in the range around 5% of the maximum intensity, where the initial rise is usually evaluated. Obviously, at higher temperatures, the slopes become smaller and therefore, the resulting apparent energy is smaller, but this may be considered to be out of the initial-rise range. As for the lower temperature range, the right-hand side of curve (b) in Fig. 4 shows that at the higher side of the $1/T$ scale, the reduction function levels-off. Obviously, this is the low-temperature range. This means that at the very low-temperature range, the evaluated activation energy is closer to the inserted 0.9 eV; this can be seen in the first two entries in Table 2. As pointed out above, this observation was made by Bräunlich (1967). From the practical point of view, it should be noted that this range of very low TL intensity is usually not measurable due to noise, and therefore, under these circumstances, the evaluated apparent activation energy may be, say, less than half the real one as mentioned above. As for the evaluated symmetry factor which, in the presented case has been 0.488, considered intermediate between first- and second-order, has also to do with the deviation of the shown straight line from curve (b) in Fig. 4. Had the dependence of the reduction function been exponential, according to Eq. (18), a first-order function would have been resulted with effective activation energy of $E - E_0$. Since the peak does not look like a first-order curve, evaluation of the frequency factor by Eq. (16) yields only some kind of effective value. However, since the effective energy is relatively small, the evaluated frequency factor can be expected to be smaller than the inserted value by several orders of magnitude, which indeed results by inserting the evaluated activation energy into Eq. (16).

The described change of the shape of the peak under these circumstances may possibly result in an effect opposite to that described by Chen and Hag-Yahya (1997) of anomalous fading. To explain this point, let us consider the lifetime of the thermal decay of the TL intensity which is (see e.g., Chen and McKeever, p. 448)

$$\tau = s^{-1} \exp(E/kT), \tag{20}$$

where T is the temperature at which the sample is irradiated and held, e.g., RT ~ 293 K. When we insert into Eq. (20) the "real" values of $E = 0.9$ eV and $s = 10^{11}$ s^{-1} we get $\tau \sim 3 \times 10^4$ s. As for the apparent value, if we insert $E_{\mathrm{eff}} = 0.46$ eV and $T_m = 424$ K into Eq. (3), we get $s_{\mathrm{eff}} = 2.4 \times 10^6$ s^{-1}. Inserting these values into Eq. (20), we get for this peak $\tau_{\mathrm{eff}} \sim 33.6$ s, about 100 times smaller than the real expected value. This may be interpreted as "anomalous stability", namely, a peak expected by the evaluated parameters to decay quickly, in fact decays much slower. Note that from the practical point of view, this anomalous behavior should not pose a severe problem simply because its occurrence may be prevented by repeating the measurement in a low enough dose such that the relevant trap will not be in saturation.

In conclusion, as pointed out, the processes involved in the study of TL and OSL are very complex and in many cases, the sets of the governing differential equations are not amenable to an analytical solution. The viable option in following these intricate processes is by simulations consisting of numerical solution of the

Table 2
Evaluated values of the activation energy at different temperatures along the initial rise range.

Initial rise temperature (K)	Activation energy (eV)
281	0.894
301	0.825
344	0.421
368	0.349

relevant sets. This is so in particular, since the experimental procedure includes at least three stages of excitation, relaxation and read-out, and sometimes many more, and the simulation by solving the relevant sets of equations involves solving them sequentially. Following an experimental procedure by such simulation is not expected to yield an analytical expression which connects physical quantities (e.g. luminescence intensity vs. dose), but it can show that certain behavior is possible within the framework of the accepted model, and even predict the occurrence of certain experimental results. Finally, as pointed out above, in some cases, a semi-analytical solution of the differential equations can be performed by using plausible simplifying approximations. When these two routes, simulation and approximation yield similar results, the validity of the conclusions is strengthened.

References

Bilski, P., Obryk, B., Olko, P., Mandowska, E., Mandowski, A., Kim, J.L., 2008. Characteristics of LiF: Mg,Cu, P thermoluminescence at ultra-high dose range. Radiat. Meas. 43, 315–318.

Bräunlich, P., 1967. Comment on the initial rise for determining trap depths. J. Appl. Phys. 38, 2516–2519.

Chen, R., 1969a. On the calculation of activation energies and frequency factors from glow curves. J. Appl. Phys. 40, 570–585.

Chen, R., 1969b. Glow curves with general-order kinetics. J. Electrochem. Soc. 116, 1254–1257.

Chen, R., Haber, G.A., 1968. Calculation of glow curves' activation energies by numerical initial-rise method. Chem. Phys. Lett. 2, 483–485.

Chen, R., Hag-Yahya, A., 1996. Interpretation of very high activation energies and frequency factors in TL as being due to competition between centres. Radiat. Prot. Dosimetry 65, 17–20.

Chen, R., Hag-Yahya, A., 1997. A possible new interpretation of the anomalous fading in thermoluminescent materials as normal fading in disguise. Radiat. Meas. 27, 205–210.

Chen, R., McKeever, S.W.S., Durrani, S.A., 1981. Solution of the kinetic equations governing trap filling. Consequences concerning dose dependence and dose-rate effects. Phys. Rev. B24, 4931–4944.

Chen, R., Pagonis, V., 2013. On the analysis of the quasi-equilibrium assumptions in the theory of thermoluminescence (TL). J. Lumin. 143, 734–740.

Dropkin, J.J., 1954. Photoconductivity in Phosphors. Final Report, Contract N6–26313. Polytechnic Institute of Brooklyn.

Dussel, G.A., Bube, R.H., 1967. Theory of TSC in a previously photoexcited crystal. Phys. Rev. 155, 764–779.

Fairchild, R.G., Mattern, P.L., Lengweiler, K., Levy, P.W., 1974. Thermoluminescence of LiF TLD-100 dosimeter crystals. IEEE Trans. Nucl. Sci. NS-21, 366–372.

Garlick, G.F.J., Gibson, A.F., 1948. The electron trap mechanism of luminescence in sulphide and silicate phosphors. Proc. Phys. Soc. 60, 394–590.

Gorbics, S.G., Attix, F.H., Pfaff, J.A., 1967. Temperature stability of CaF_2:Mn and LiF (TLD-100) thermoluminescent dosimeters. Int. J. Appl. Radiat. 18, 625–630.

Haake, C.H., 1957. Critical comment on a method for determining electron trap depths. J. Opt. Soc. Am. 47, 649–652.

Halperin, A., Braner, A.A., 1960. Evaluation of thermal activation energies from glow curves. Phys. Rev. 117, 408–415.

Hickmott, T.W., 1972. Thermoluminescence and color centers in rf-sputtered SiO_2 films. J. Appl. Phys. 43, 2339–2351.

Hoogenstraaten, W., Klasens, H.A., 1953. Some properties of zinc sulfide activated with copper and cobalt. J. Electrochem. Soc. 100, 366–375.

Kelly, P.J., Bräunlich, P., 1970. Phenomenological theory of TL. Phys. Rev. B1, 1587–1595.

Mandowski, A., 2006. Topology-dependent thermoluminescence kinetics. Radiat. Prot. Dosim. 119, 23–28.

Obryk, B., Bilski, P., Olko, P., 2011. Method of thermoluminescent measurement of radiation doses from micrograys up to a megagray with a single LiF: Mg, Cu, P detector. Radiat. Prot. Dosim. 144, 543–547.

Pohlit, W., 1969. Thermoluminescence in LiF. I. Measurement of activation energy of electrons in different traps. Biophysik 5, 341–350.

Randall, J.T., Wilkins, M.H.F., 1945. The phosphorescence of various solids. Proc. Roy. Soc. Lond. A184, 347–365.

Sunta, C.M., Feria, A.W.E., Piters, T.M., Watanabe, S., 1999. Limitation of peak fitting and peak shape methods for determination of activation energy of thermoluminescence glow peaks. Radiat. Meas. 30, 197–201.

Taylor, G.C., Lilley, 1978. The analysis of thermoluminescence glow peaks in LiF (TLD-100). J. Phys. D. Appl. Phys. 11, 567–581.